**Article:**
Ghavam, S., Garcia-Garcia, G. and Styring, P. (2021) A novel approach to ammonia synthesis from hydrogen sulfide. International Journal of Hydrogen Energy, 46 (5). pp. 4072-4086. ISSN: 0360-3199

https://doi.org/10.1016/j.ijhydene.2020.10.192

INTERNATIONAL JOURNAL OF HYDROGEN ENERGY 46 (2021) 4072–4086

Available online at www.sciencedirect.com

ScienceDirect

journal homepage: www.elsevier.com/locate/he

# A novel approach to ammonia synthesis from hydrogen sulfide

*Seyedehhoma Ghavam*[*], *Guillermo Garcia-Garcia*, *Peter Styring*

*Department of Chemical & Biological Engineering, The University of Sheffield, UK*

## HIGHLIGHTS

- Ammonia can be produced from hydrogen sulfide via membrane technology.
- The proposed process consumes less water compared to a water electrolyzer.
- Small physical footprint with fewer process steps compared to other processes.
- This process does not produce pollutants.
- The process is energy intensive compared to other ammonia production technologies.

## GRAPHICAL ABSTRACT

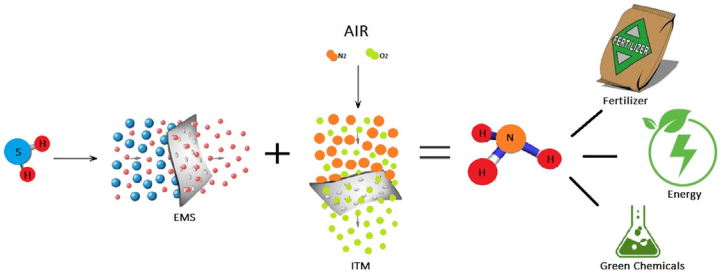


## ARTICLE INFO

*Article history:*
Received 30 August 2020
Received in revised form
7 October 2020
Accepted 22 October 2020
Available online 27 November 2020

*Keywords:*
Ammonia
Hydrogen sulfide
Electrochemical membrane separation
Solid state ammonia synthesis

## ABSTRACT

There are a number of shortcomings for currently-available technologies for ammonia production, such as carbon dioxide emissions and water consumption. We simulate a novel model for ammonia production from hydrogen sulfide through membrane technologies. The proposed production process decreases the need for external water and reduces the physical footprint of the plant. The required hydrogen comes from the separation of hydrogen sulfide by electrochemical membrane separation, while the required nitrogen is obtained from separating oxygen from air through an ion transport membrane. 10% of the hydrogen from the electrochemical membrane separation along with the separated oxygen from the ion transport membrane is sent to the solid oxide fuel cell for heat and power generation. This production process operates with a minimal number of processing units and in physical, kinetic, and thermal conditions in which a separation factor of ~99.99% can be attained.

*Abbreviations:* FAO, Food and Agriculture Organization; GHG, Green House Gas; SOFC, Solid Oxide Fuel Cell; SSAS, Solid State Ammonia Synthesis; ITM, Ion Transport Membrane; EMS, Electrochemical Membrane system; PSA, Pressure Swing Adsorption; VBA, Visual Basic for Applications; ODE, Ordinary Differential Equation; CHP, Combined Heat and Power; PDE, Partial Differential Equation; CapEx, Capital Expenditure.

* *Corresponding author.*
E-mail address: sghavam1@sheffield.ac.uk (S. Ghavam).

https://doi.org/10.1016/j.ijhydene.2020.10.192

Ion transport membrane
Fertilizer



## Introduction

By 2050, global food production will need to increase by 70% in order to keep up with the worldwide growth in population [1]. Commercial fertilizers are used in about 40–60% of global food production with the main feedstock for their production processes being fossil fuels [2]. Alexandratos & Bruinsma projected that fertilizer usage will increase proportionally to the population growth in the period 1960–2050 [3]. Furthermore, they estimated that fertilizer usage will increase by approximately 25% from 210 million tonnes (Mt) in 2020 to 262 Mt in 2050.

With a global production of 146 Mt reported in 2016, ammonia ($NH_3$) is second to sulfuric acid ($H_2SO_4$) in production volume for the manufacturing of fertilizers [4,5]. Industrially, ammonia can also be utilized in a wide range of applications, from the production of polyimides and nitric acid, to its use as an energy carrier for energy storage and transportation [5]. Ammonia consists of 17.6 wt percent (wt%) hydrogen, showing that ammonia is an indirect hydrogen storage compound [6]. The exothermic reaction between hydrogen and nitrogen results in the production of ammonia, via the following chemical reaction 1:

$$\frac{1}{2}N_2(g)+\frac{3}{2}H_2(g) \rightarrow NH_3(g)\ \Delta H = -93(KJ/mol) \quad \text{(R1)}$$

Ammonia is generally produced via the Haber-Bosch process in vast production facilities in volumes of approximately 1000–1500 t/day [4]. Fossil fuels are the main feedstock for 90% of the ammonia produced globally through the Haber-Bosch process [7]. This process typically operates in the presence of an iron-based catalyst at a temperature in the range of 400–500 °C and pressure in the range of 150–300 bar [8,9]. The production of ammonia via the Haber-Bosch process requires hydrogen, of which 96% is currently derived from fossil fuels [10]. This process consumes approximately 3–5% of the global natural gas supply [9], which corresponds to 1–2% of the global energy supply [7,9].

The Steam Methane Reforming (SMR) process produces 72% of the global hydrogen used for ammonia production, while coal produces 26% [11]. A standard SMR process typically produces approximately 9–10 t of carbon dioxide equivalents ($CO_2e$) for every t of hydrogen produced [10]. Overall, the Haber-Bosch process generates very large greenhouse gas (GHG) emissions (>2.16 kg $CO_2$/kg $NH_3$). This is a very significant drawback of the Haber-Bosch process.

Approximately 70–90% of ammonia manufacturing costs are directly tied to the price of natural gas [12]. Fluctuations in the price of ammonia are usually tied to volatility in natural gas prices. The price of both natural gas and ammonia have increased every year, the former from approximately 4 \$/1000 $ft^3$ in 1975 to 15 \$/1000 $ft^3$ in 2015, and the latter from 290 \$/t of $NH_3$ in 1975 to approximately 850 \$/t of $NH_3$ in 2015. Between 2012 and 2016, the price of natural gas decreased globally due to the increase in natural gas production, mainly in the US [13].

The main challenge for the production of ammonia is finding an economically-viable, energy-efficient, and environmentally-friendly approach to produce hydrogen. The most widely adopted technology for sustainable ammonia production is water electrolysis powered by renewable technologies, such as wind and solar. Generally, a continuous supply of pretreated water with high purity levels is required for the operation of a water electrolyzer. Furthermore, 9 t of water is required for the production of 1 t of hydrogen. In 2016, the amount of ammonia produced was reported to be 146 Mt globally [14]. Based on this data, for the production of the same amount of ammonia through water electrolysis, 233.6 Mt of water is required. Significant increases in water scarcity in the next few decades, leading to problems such as food security, environmental sustainability, and negative economic growth, were shown in a number of studies, e.g. Ref. [15–17]. As hydrogen is a key factor for all ammonia production processes, it is paramount to have access to a steady supply of this gas. Pilot trials are already being developed to evaluate the viability of hydrogen-gas pipeline supplies. For example, Cadent Gas Ltd., in the UK, is in the early stages of the Liverpool-Manchester Hydrogen Cluster project to introduce hydrogen in the gas network in the Liverpool-Manchester area. The initial conceptual stage is complete and further developments are underway [18].

**Nomenclature**

| | |
|---|---|
| wt % | Weight percent |
| FE (%) | Faradaic efficiency (%) |
| $J$ | Oxygen flux |
| $E_{cell}$ | Cell over-potential |
| $\eta_{act}$ | Activation over-potential |
| $\eta_{conc}$ | Concentration over-potential |
| $E_{eq}$ | Equilibrium over-potential |
| $IR_{cell}$ | Ohmic over-potential |
| $E_{ner}$ | Nernst potential |
| $\alpha$ | Transfer coefficient |
| $r_{NH3}$ | Ammonia reaction rate |
| $R$ | Universal gas constant |
| $I$ | Total current |
| $V$ | Total voltage |
| i | Current density |
| $\delta$ | Membrane thickness |
| $\sigma$ | Membrane conductivity |
| $T$ | Operational temperature |
| $i_o$ | The exchange current density |

**Table 1 – A comparison of various hydrogen sulfide separation methods.**

| Process | Brief description | Advantages | Disadvantages |
|---|---|---|---|
| Absorption | Absorption is a process in which the component existing in the gas phase (hydrogen sulfide) transitions into the liquid phase by passing through a boundary phase. | Mature technology, possible to regenerate the solution, high removal rate, operates at room temperature, ease of operation, and low maintenance costs. | The mixture of hydrogen sulfide in solvent is problematic, large amounts of solvent is required, high energy costs (related to the regeneration of the solvent, pumping, and gas compression, etc.), significant initial installation costs, and high liquid-gas ratio for high removal efficiency. |
| Adsorption | Adsorption is a process through which molecules of sulfur are retained by physical/chemical forces existing on the surface of a porous solid which acts as an adsorbent. Examples of a modern adsorbent include Metal Organic Frameworks (MOFs) [25] and Covalent Organic Frameworks (COFs) [26]. | Mature technology, efficient for low contaminant levels, operates under ambient conditions, and has a simple mechanical design. | Significant operating costs, reduction of removal efficiency after regeneration, not all adsorbent can be regenerated, low adsorption capacity/unit of area of an adsorbent, regeneration of solid adsorbent takes place at high temperatures. |
| Membrane | Separation through membranes are based on gas diffusion. The membranes are comprised of thin barriers made up of different materials (polymers, zeolite, etc.) which monitor passage of certain materials through them. | Mature technology, low chemical consumption, low environmental impact, high removal efficiency, small physical footprint, low operating costs, and the separated byproducts do not contain pollutants. | High operational cost, high energy demand due to high operational temperatures to achieve high purity levels, some solvents may cause degradation of membrane, and can be easily contaminated. |
| Separation | This process is based on the conversion of hydrogen sulfide into hydrogen and elemental sulfur. Porous liquids allow selective dissolving and separation of $H_2S$ providing a more energy efficient method of separation compared to conventional amine solvents [27]. | Mature technology (Clause process), low environmental impact, and the separated byproducts do not contain pollutants. | Significant initial installation costs, and to remove high volumes of hydrogen sulfide, requires on site installation |

Hydrogen can be produced from other chemicals, such as hydrogen sulfide ($H_2S$). Hydrogen sulfide is toxic, hazardous, and highly flammable under normal conditions and becomes explosive when it is mixed with air. Significant work has been carried out to reduce hydrogen sulfide to ppm levels before it can be used in applications such as for the production of sulfuric acid and in fuel cells [19,20]. Annually, over 12 Mt of hydrogen sulfide is produced in the US as a byproduct of industrial activities [20]. When a fuel is reformed, gasified or digested, sulfur appears in the form of hydrogen sulfide [21]. Hydrogen sulfide has a number of industrial uses, with the main application being the production of sulfuric acid and elemental sulfur [22]. This chemical compound can be commercially obtained through two different methods: (1) capture from gas mixtures and chemical means, and (2) capture from natural gas and gases that are related to crude oil production, which are comprised of different levels of hydrogen sulfide, from trace to high amounts (70–80%) [22]. There are also a number of companies that purify hydrogen sulfide at different levels and transport it in high volumes (>1500 gal/day) with specific handling conditions to ensure safety. There are many routes for separating hydrogen sulfide from carbon-based gases, of which many are inefficient or produce other pollutants as their byproducts. Moreover, some of these methods are multistage processes that require large capital investments [23,24]. Table 1 shows different processes for hydrogen sulfide separation along with their advantages and disadvantages. One of the main advantages of membrane technology over other upgrading processes mentioned in Table 1 is that it converts hydrogen sulfide into pure hydrogen, which is the main feedstock for our ammonia production process. At the same time, apart from elemental sulfur, which can be sold commercially, no pollutants are produced in the conversion of hydrogen sulfide into pure hydrogen.

1 kg Green Ammonia with SOFC and without CO2 Utilization (of project Light).

In this context, the aim of this paper is to propose a novel synthesis process to produce ammonia from hydrogen sulfide through a carbon-free process with low water utilization and a minimal number of operating stages. An overview of the process is presented in Section Overview of the proposed synthesis process, the modelling method used is explained in Section Modelling method, the processing units are detailed in Section Processing units, the mass and energy balances are shown in Sections Mass balance results and Energy balance results, and finally the main conclusions from this work are presented in Section Conclusions.

## Overview of the proposed synthesis process

We propose a novel model for ammonia production from hydrogen sulfide through a series of compact processes (membranes). In this method, compressed air enters an Ion Transport Membrane (ITM) for oxygen separation. The resulting oxygen is routed to a Solid Oxide Fuel Cell (SOFC). The remaining nitrogen after oxygen separation is divided into two streams: one stream is directed to an Electrochemical Membrane Separation (EMS) process as sweep gas and the other stream goes to Solid State Ammonia Synthesis (SSAS) as a feedstock for ammonia production.

The hydrogen needed for ammonia synthesis is separated from hydrogen sulfide by EMS. Hydrogen sulfide is converted into hydrogen and sulfur in the presence of a sweep gas (nitrogen) which is the byproduct from the ITM. The hydrogen along with the nitrogen from the ITM enter the SSAS proton ($H^+$) conducting membrane for ammonia production. 25% of the hydrogen from EMS is fed into a SOFC for generating heat, power, and steam for the entire process.

The process flow diagram of the proposed production process is shown in Fig. 1. Each of the numbers shown in Fig. 1 correspond to a specific processing unit incorporated in the proposed process. These process steps are described, along with their mathematical modelling results in Section 4.

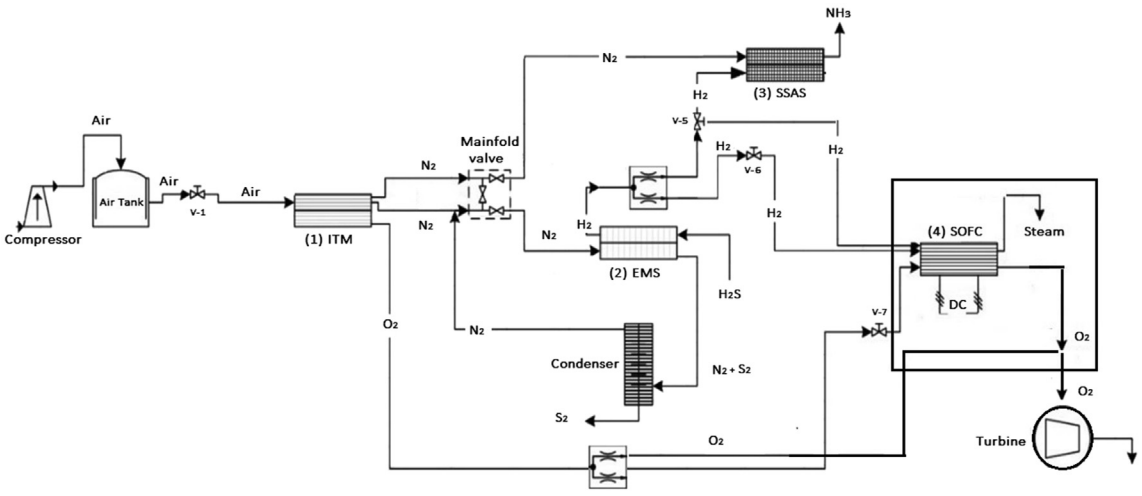


**Fig. 1 – Schematic of the process flow diagram of the proposed ammonia production process.**

## Modelling method

The aim of this study is to analyze the GHG emissions, energy, and water usage through a novel process for the production of ammonia from hydrogen sulfide. This is done by developing a mathematical model with mass and energy balance equations to simulate the performance of the ammonia production process with Visual Basic for Applications (VBA) (embedded in Microsoft Excel). The input and output functions of the model are written in VBA and the results are linked to Microsoft Excel. The mass and energy balances of this simulated model are assessed in various physical and chemical conditions (i.e. temperature, pressure, flow rates, specific heat capacity, thermal conductivity, effectiveness of the heat exchangers, heat loss, drive motor power of the compressor, porosity, tortuosity, flux, and permeability of the membranes, etc.) and sizing of various processing units (i.e. thickness, length, area, number of tubes and modules, etc.). This is done by using the assumptions and mathematical equations (mass transfer, energy transfer, thermodynamics, and kinetics) which are determined for each processing unit. Since the entire process operates sequentially, the output and the performance of each component affects the input of the other components, except for the ITM which is the initial processing unit of this proposed process. The modelling approach selected for this model is a combination of equation oriented and sequential modular approach, i.e., the components (processing units) are modelled in sequence, starting with the feed stream as well as the entire process flow which is treated as a set of mathematical equations that need to be solved simultaneously.

The following assumptions were made to create the mathematical model:

- All gases are in an ideal state ($PV = nRT$)
- The input gas flow enters the process at ambient temperature (25 °C) and pressure (1 atm)
- The ideal gases are compressed adiabatically
- The process operates at a steady state condition
- There is no leakage (no heat and material loss)
- Hydrogen sulfide is 99.99% pure when entering the EMS
- This proposed production process is powered by renewable energy sources

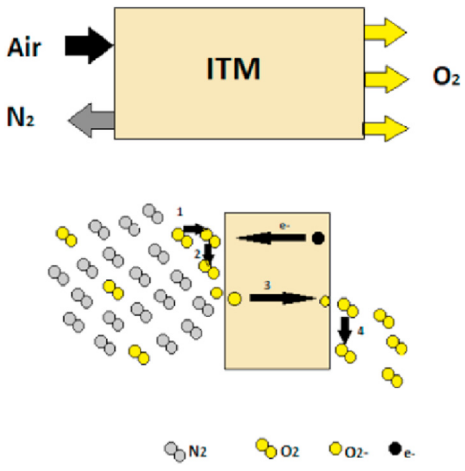


**Fig. 2 – A schematic of the ITM separation process.**

The materials utilized for different types of membranes in the proposed process are shown in Table 2.

## Processing units

This section describes the processing units used to model the synthesis of ammonia from hydrogen sulfide: ITM, EMS, SSAS, and SOFC.

### *Ion transport membrane (ITM) for oxygen separation (1)*

This process consists of an ITM for oxygen separation from air. This membrane generally operates at temperatures of 800–900 °C and pressures of 10–30 bar [31]. ITM generally consists of mixed ion and electron-conducting ceramic materials with high oxygen separation selectivity. There is no need to apply a voltage to this system as membrane materials have the capability to conduct the electrons and oxygen ions from high to low pressure. This membrane is an innovative technology for air separation which has a simple configuration with a lower energy penalty when compared to mature technologies currently in use such as cryogenic distillation. A schematic of ITM can be seen in Fig. 2, which shows that oxygen molecules pass the membrane, while the nitrogen molecules do not pass and accumulate behind the membrane.

**Table 2 – Different materials for membranes used in the proposed production process.**

| Processing unit | Material composition | Chemical reaction | References |
|---|---|---|---|
| Ion Transport Membrane (ITM) | $SrCo_{0.9}Sc_{0.1}O_{3-\delta}$ | Non permeate side: $½\ O_2 + 2e^- \rightarrow O^{2-}$<br>Permeate side: $O^{2-} \rightarrow ½\ O_2 + 2e^-$ | [28] |
| Electrochemical Membrane Separation (EMS) | Cathode: $Gd_2Ti_{2-x}Mo_xO_7$ (x = 0.0–2.0),<br>Electrolyte: $La_{0.7}Sr_{0.3}VO_3$<br>Anode: NiO | Cathode: $H_2S + 2e^- \rightarrow H_2 + S^{2-}$<br>Anode: $S^{2-} \rightarrow ½\ S + 2e^-$<br>The overall reaction: $H_2S \rightarrow ½\ S_2 + H_2$ | [21] |
| Solid State Ammonia Synthesis (SSAS) | Cathode: $SmFe_{0.7}Cu_{0.3-x}Ni_xO_3$ (x = 0–0.3) (SFCN)<br>Electrolyte: Nafion (membrane)<br>Anode: Ni-doped SDC (Ni-SDC) $NiO–Ce_{0.8}Sm_{0.2}O_{2-\delta}$ | Cathode: $N_2 + 6H^+ + 6e^- \leftrightarrow 2NH_3$<br>Anode: $3H_2 \leftrightarrow 6H^+ + 6e^-$<br>Overall reaction: $N_2 + 3H_2 \leftrightarrow 2NH_3$ | [29] |
| Solid Oxide Fuel Cell (SOFC) | Cathode: $La_{1-x}Sr_xMnO_3$, (LSM)<br>Electrolyte: YSZ<br>Anode: Ni-YSZ composite | Cathode: $½\ O_2 + 2e^- \rightarrow O^{2-}$<br>Anode: $H_2 + O^{2-} \rightarrow H_2O + 2e^-$<br>Overall reaction: $½\ O_2 + H_2 \rightarrow H_2O$ | [30] |

**Table 3 – A comparison of different types of air separation technologies (cryogenic and non-cryogenic) [33].**

| | Ion transport membrane (ITM) | Polymeric membranes | Cryogenic air separation | Pressure Swing adsorption (PSA) and vacuum Swing adsorption (VSA) |
|---|---|---|---|---|
| Production capacity | ≥100 t/day | <20 t/day | >3000 t/day | Plant size is up to about 56.7 t/day |
| Purity level | 99–100% | ~40% | 99+ | 95% |
| Current status | Semi-Mature | Mature | Mature | Mature |
| Description | This membrane is a solid inorganic oxide ceramic material that transports oxygen ions at high pressures (10–30 bar) and temperatures (800–900 °C). | The membrane system is based on the variance between particle diffusion rates throughout the membrane. The main drawback is its low chemical resistance. | The technology is based on the fact that each of the components that make up air have different boiling points. This process operates at a temperature of approximately 185 °C. | Under pressure, gases tend to be adsorbed to solid surfaces. As the pressure increases, the adsorption rate increases and as the pressure decreases the gas is desorbed and released. |
| Advantages | Simple in design, low energy penalty, low cost, high tonnage, and low environmental impact. | Flexibility in scale (due to modularity), and a mature and well-developed technology. | The most mature and well-developed technology, cost effective, and efficient. | Mature and well-developed technology, continuous oxygen production, capable of maintaining a high purity level of 99%, low capital costs, flexible design for different adsorbents. |

A comparison of different types of air-separation technologies (cryogenic and non-cryogenic) is shown in Table 3. The purity level of oxygen resulting from ITM is higher than polymeric membranes, Pressure Swing Adsorption (PSA), and Vacuum Swing Adsorption (VSA) with 99–100% purity level. However, the purity level of the resulting oxygen from ITM is almost the same as cryogenic air separation. Since the physical footprint of this processing unit (ITM) is small compared to cryogenic air separation, it is a suitable option for our proposed process. The separated nitrogen required for this proposed ammonia production process must reach a purity level higher than 99% in order to be utilized in the SSAS. Nitrogen with purity levels lower than 99% that contain trace amounts of oxygen cause irreversible poisoning of the catalyst in the SSAS [32].

The input and output data of ITM is presented in Table 4. The oxygen permeate pressure control, cell temperature and pressure operate in a specific range and were obtained from literature data such as Han et al. [31] and Sun et al. [28] and the values were selected specifically based on our design constraints. The air flow rate (oxygen and nitrogen flow rates) changes based on the amount of ammonia produced, while the inner and outer radius, and tube length of the membrane are also subject to change accordingly [28]. Changing each of the mentioned input parameters will result in different output values. The output from ITM can be separated into two streams. The resulting oxygen is routed to SOFC, while the nitrogen is divided into two streams: one stream enters the EMS as the sweep gas and the other stream enters the SSAS to produce ammonia.

The oxygen flux and permeability of the ITM were calculated using Eq. 1 and Eq. 2, where $J$ is the oxygen flux. The driving force variable in Eq. 2 is the pressure difference at the feed side and permeate side.

$$J = \frac{Molar\ flow\ rate}{Area}\ \left(mol\ s^{-1}m^{2}\right) \tag{1}$$

$$Permeability = \frac{J \times Thickness}{driving\ force}\ \left(mol\ m^{-1}s^{-1}atm^{-1}\right) \tag{2}$$

### *Electrochemical membrane separation (EMS) for hydrogen sulfide removal (2)*

The upgrading stage used in the proposed process for removing hydrogen sulfide is an EMS system. Via this method, hydrogen sulfide is removed in one continuous phase at temperatures of 600–700 °C, which leads to the production of elemental sulfur. A schematic of EMS is shown in Fig. 3.

In the EMS, hydrogen sulfide is removed from the fuel gas stream and is converted to pure hydrogen, which is the main feedstock for ammonia production. The sulfur by-product can be sold commercially to industries involved in the production of sulfuric acid, agricultural industries for fertilizer production, etc. There are seven steps required for electrochemical removal of hydrogen sulfide: (1) gaseous diffusion of hydrogen sulfide to the electrode, (2) hydrogen sulfide diffusion through the electrode pores to the electrolyte-electrode interface, (3) adsorption and reduction of hydrogen sulfide at the cathode surface, (4) production of a sulfide ion, (5) migration and

**Table 4 – The input and output data of the ITM.**

| ITM Input data | | | ITM Output data | | |
|---|---|---|---|---|---|
| Parameters | Data | Units | Parameters | Data | Units |
| Air flow rate | 37,368.240 | Kg/day | Diffusivity of oxygen vacancy | 5.959E-06 | $cm^2/s$ |
| Oxygen flow rate | 7847.33 | Kg/day | Forward reaction rate | 1.647E-05 | $cm^2/atm^{0.5}.s$ |
| Nitrogen flow rate | 29,520.91 | Kg/day | Reverse reaction rate | 5.778E-07 | $mol/atm^{0.5}.s$ |
| Cell temperature | 850 | °C | Oxygen permeation flux | 1.679E-07 | $mol/cm^2.s$ |
| Cell pressure | 10 | atm | Required cell area | 1.690 | $m^2$ |
| Outer radius | 10 | mm | Number of tubes | 1346 | N° |
| Inner radius | 0.115 | mm | Number of modules | 67 | N° |
| Tube length | 20 | cm | Membrane thickness δ | 2.214 | mm |
| Number of tubes/number of modules | 20 | N° | Oxygen pressure at permeate side | 0.3 | atm |
| Oxygen permeate pressure control π (Limits:5 < π < 7) | 7 | | Permeance | 1.731E-08 | $mol/cm^2.s.atm$ |
| | | | Permeability | 3.832E-09 | mol/cm.s.atm |
| | | | Conductivity | 1.691E-01 | S/cm |
| | | | Total voltage | 59.867 | Volt |
| | | | Total power | 9.0286 | kW |

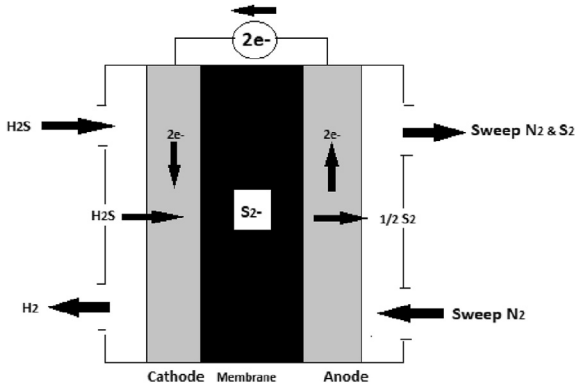


**Fig. 3 – A schematic of an EMS.**

diffusion of sulfide ions through the electrolytic membrane, (6) oxidation of sulfide ions to elemental sulfur at the anode, and (7) diffusion of sulfur away into the bulk purge stream. This process works continuously and takes place in one step, making the technology economical due to lower costs associated with manpower and operation [34]. An efficient design of the cell stack ensures that the physical footprint of the plant is kept to a minimum [34].

The electrolytic cell has the following basic components: (1) cell housing, (2) an inert ceramic membrane, (3) an electrolyte, (4) an anode, and (5) a cathode. The chemical reactions that occur in an EMS are as follows:

Hydrogen sulfide is passed through the cathode, as shown in reaction 2:

$$H_2S + 2e^- \rightarrow H_2 + S^{2-} \quad \text{(R2)}$$

Reaction 3 shows the transport of sulfide ions throughout the membrane to the anode side:

$$S^{2-} \rightarrow \tfrac{1}{2} S_2 + 2e^- \quad \text{(R3)}$$

The overall reaction resulting from both reactions taking place in the anode and cathode at the temperature of 650 °C is (reaction 4):

$$H_2S \rightarrow \tfrac{1}{2} S_2 + H_2 \quad \text{(R4)}$$

The input and output data of the EMS is shown in Table 5. Membrane temperature, pressure, and applied voltage operate in a specific range and were obtained from literature data such as Burke et al. [34] and the values were selected specifically based on our design constraints. Hydrogen sulfide flow

**Table 5 – The input and output data of the EMS.**

| EMS Input data | | | EMS Output data | | |
|---|---|---|---|---|---|
| Parameters | Data | Units | Parameters | Data | Units |
| Hydrogen sulphide flow rate | 10,000 | Kg/day | $S_2$ vapor flow rate out | 9411.76 | Kg/day |
| Inlet gas temperature | 25 | °C | $N_2$+$S_2$ flow rate out | 36,437.038 | Kg/day |
| Inlet gas pressure | 1 | Atm | $H_2$ flow rate out | 588.235 | Kg/day |
| Membrane temperature | 650 | °C | Maximum $H_2S$ removal flux | 1.7616E-05 | $gm/cm^2.s$ |
| Membrane tortuosity Ƭ | 3.6 | | Mass transfer limited current density | 3.399 E+00 | $mA/cm^2$ |
| Membrane thickness | 3 | Mm | Total applied current | 3.760 E+03 | A |
| Membrane surface area | 3000 | $cm^2$ | Total voltage/Cell | 1.143 | volt |
| Membrane porosity | 36 | % | Required cell power | 475.320 | kW |
| Mass transfer coefficient ($K_m$) | 11 | cm/s | Number of cells | 111 | N° |
| Electrolyte diffusivity | 1.00E-05 | $cm^2/s$ | | | |
| Electrolyte average density | 5.450 | $mol/cm^3$ | | | |
| Applied voltage | 0.75 | volt | | | |

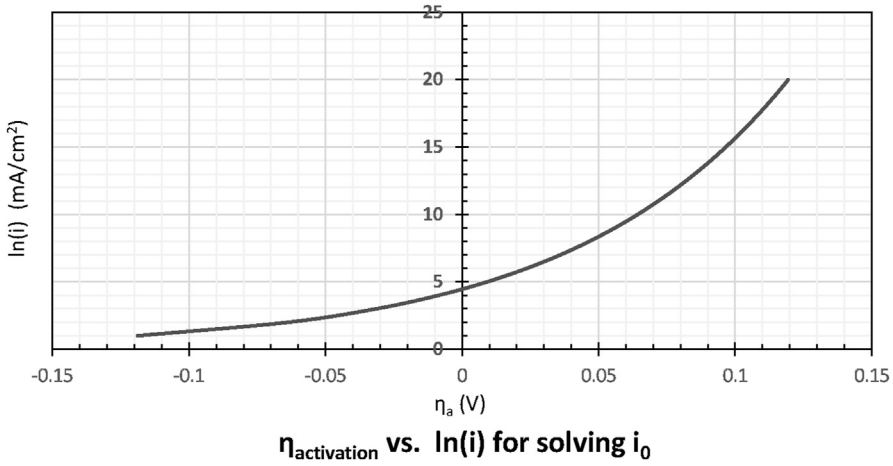


**Fig. 4 – ln (i) versus activation voltage for EMS.**

rate can be changed based on the amount of hydrogen required for ammonia synthesis and the thickness and surface area of the membrane are also subject to change accordingly [34]. Changing each of the mentioned input parameters will result in different output values. The output hydrogen from the EMS is separated into two streams. The first stream, which is comprised of 90% of the hydrogen is routed to SSAS for ammonia production, while the second stream containing the remaining hydrogen enters SOFC for heat and power production. This EMS operates at a temperature of 650 °C and atmospheric pressure. 10 t/day of hydrogen sulfide is required to produce 3 t of ammonia per day. For running this system with 3.6 tortuosity and porosity of 36% with the given dimension (thickness of 3 mm per cell and total surface area of 3000 $cm^2$), 475.320 kW power is required.

In order to solve the Butler-Volmer equation, a Tafel approximation was carried out based on Eq. 3. $\eta_a$ is the activation overpotential (V), $T$ is membrane's operational temperature (K), $R$ is the universal gas constant (J/mol.K), $F$ = Faraday's constant, $\alpha$ = the transfer coefficient, $i_o$ = the exchange current density, and $i$ = the current density.

$$\eta_a = \frac{RT}{\alpha F} ln \frac{i}{i_o} = \frac{RT}{\alpha F} lni_o + lni \tag{3}$$

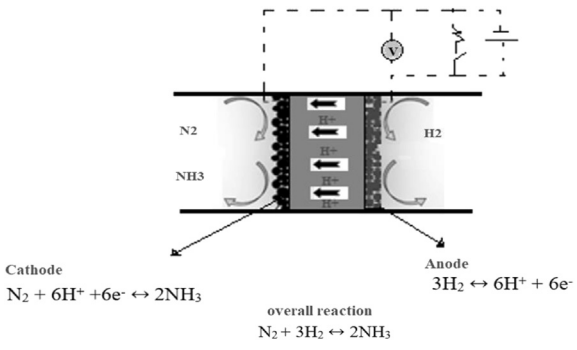


**Fig. 5 – A schematic of a solid-state ammonia synthesis device; via a proton conducting electrolyte [32].**

$i$ versus $\eta_a$ was plotted in order to find $i_o$ at the intersection of (i) axis, as shown in Fig. 4 $i_o$ was found to be ~4.5 mA/$cm^2$.

### *Solid State Ammonia Synthesis (SSAS) for ammonia production (3)*

There are several issues associated with the catalytic process for ammonia synthesis (Haber Bosch) such as low conversion efficiency, severe environmental pollution, and high energy usage. These problems are addressed here by utilizing a SSAS [35]. The overall chemical reaction that takes place in the cell for ammonia production is divided into two electrode reactions. Each of the reactions takes place at one of the electrodes. The exact form of the electrode reactions is related to the type of electrolyte: either a $H^+$ ion conductor or an $O_2$ ion conductor. Moreover, the source of $H^+$ can be hydrogen or water. For a cell based on a $H^+$ conducting electrolyte, the reactions that take place in the electrodes are as follows (reaction 5 and 6) [36]:

Anode:

$$\frac{3}{2}H_2 \rightarrow 3H^+ + 3e^- \tag{R5}$$

Cathode:

$$\frac{1}{2}N_2 + 3H^+ + 3e^- \rightarrow NH_3 \tag{R6}$$

A schematic of a proton-conducting membrane along with the chemical reactions taking place inside the cells are shown in Fig. 5. The cell is comprised of a solid-state $H^+$ conductor. Two porous metal films are located on the two sides of the solid electrolyte and function as electrodes. Hydrogen migrates throughout the electrolyte in the form of $H^+$ to the cathode where the half-cell reaction occurs [32].

All studies on electrochemical ammonia production are divided into two categories based on the operational temperature range of the electrochemical cell: temperatures lower than 100 °C are considered low temperature while temperatures in the range of 400–750 °C are considered high temperatures [35]. According to Soloveichk [4], the advantages of the

**Table 6 – The input and output data of the SSAS.**

| SSAS Input data | | | SSAS Output data | | |
|---|---|---|---|---|---|
| Parameters | Data | Units | Parameters | Data | Units |
| Inlet temperature | 80 | °C | Produced $NH_3$ | 3030.30 | kg/day |
| Inlet pressure | 1 | Atm | $N_2$ out | 0.001 | kg/day |
| Electrode conductivity (σ) | 0.036 | 1/cm.ohm | Maximum Reaction Rate/Electrode | 1.13E-08 | mol/s. $cm^2$ |
| Membrane surface area | 1.95 | $cm^2$ | Actual reaction rate | 3.080E-06 | mol/s. $cm^2$ |
| Membrane thickness (δ) | 0.010 | Cm | Required area | 6.697 E+05 | $cm^2$ |
| | | | Number of cells | 34 | N° |
| | | | Cell power | 0.0012 | kW |
| | | | Faradaic efficiency | 99 | % |

electrochemical technology compared to thermochemical (Haber Bosch) are:

1 Higher efficiency allowing greater energy saving
2 Reduced amount of purification needed due to higher selectivity
3 Reduced Capital Expenditure (CapEx) costs thanks to lower temperatures and pressures
4 Suitability for small to medium scale utilization thanks to the linear scalability of these plants

One of the major disadvantages of high-temperature electrochemical ammonia synthesis is that it can decompose thermally after being produced. This issue is addressed in our proposed study by incorporating a low-temperature SSAS into the proposed production process by using the same material and operational conditions (temperature and pressure) as in the study by Xu et al. [29]. The study examined a maximum ammonia production rate of $1.13 \times 10^{-8}$ mol.$s^{-1}$. $cm^{-2}$ operating at a low temperature of 80 °C with an applied voltage of 2 V by using a Nafion membrane (as the electrolyte), a Ni-samaria-doped ceria (Ni-SDC) NiO–$Ce_{0.8}Sm_{0.2}O_{2-\delta}$ anode and a $SmFe_{0.7}Cu_{0.3-x}Ni_xO_3$ (x = 0–0.3) (SFCN) cathode, and by using hydrogen and nitrogen as the reactants, operating at atmospheric pressure. In this study a high Faradaic efficiency of 90.4% was attained. This figure is higher when compared to other studies, when testing low-temperature ammonia synthesis processes.

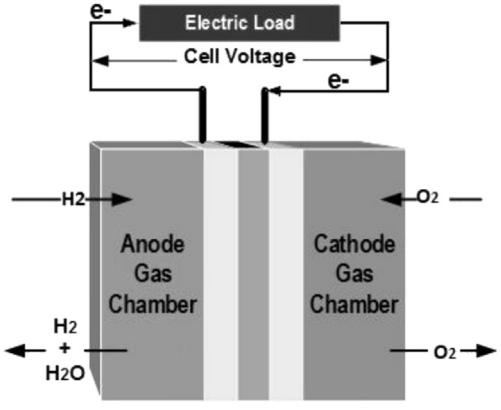


**Fig. 6 – A schematic of SOFC.**

The input and output data resulting from the modelling in VBA is presented in Table 6. The electrode conductivity and inlet temperature were obtained from literature data such Garagounis et al. [8] and the values were selected specifically based on our design constraints. The surface area and thickness of the membrane are also subject to change [29]. By changing the mentioned values in the input parameters, the following output results were obtained. For producing approximately 3 t of ammonia per day, 29,520.91 kg/day nitrogen and 534.76 kg/day of hydrogen are required. 1996.522 kW power is needed to run this system. This membrane operates at a temperature of 80 °C and at atmospheric pressure.

The empirical formula based on our simulated model shows that the relation between the input hydrogen sulfide flow rates (kg/day) to the output flow rate of ammonia being produced (kg/day) is: Y = 0.303 X + 6E-06.

There is a proportional relationship between the reaction rate and cell current density as shown in Eq. 4. $r_{NH3}$=ammonia reaction rate, $E_{ner}$ = Nernst voltage, $E_{cell}$ = applied voltage, σ = membrane conductivity, and δ = membrane thickness.

$$r_{NH_3} = \frac{E_{ner} - E_{cell}}{\left(\delta/\sigma\right)6F} \quad (4)$$

***Solid oxide fuel cell (SOFC) for heat and power production (4)***

In our proposed system a fuel cell is used for steam and electricity generation. Fuel cells are competitive sources of power since they have a number of advantages, such as high efficiency, flexibility in their usage, and lack of noise [37]. They can also be used in an extensive range of operating temperatures; this means that they are capable of being used in multiple applications. SOFC operates at 700–1000 °C. These temperatures are higher than for other types of fuel cells, are the reason for its use in power generation and hybrid power applications [38]. This fuel cell was selected mainly due to its ability to generate up to 3 MW power when compared to other types of fuel cells [39]. A schematic of an SOFC is shown in Fig. 6.

The SOFC reactions are:

Anode

$$H_2 + 1/2O_2^{-2} \rightarrow H_2O + 2\,e^- \quad (R7)$$

Cathode

**Table 7 – The input and output data of the SOFC.**

| SOFC Input data | | | SOFC Output data | | |
|---|---|---|---|---|---|
| Parameters | Data | Units | Parameters | Data | Units |
| Cell temperature | 1000 | °C | Total number of cells | 416 | N° |
| Cell pressure | 1 | atm | Number of stacks | 4 | N° |
| Ionic conductivity | 0.05 | 1/cm.ohm | Total current | 122.012 | Amp |
| Electrolyte thickness (δ) | 200 | μm | Oxygen flux | 3.16E-07 | mol/s.cm$^2$ |
| Cell area | 1000 | cm$^2$ | Total voltage | 322.22 | volt |
| Number of fuel cells/stack | 100 | N° | Total current density | 50.760 | A/cm$^2$ |
| Applied voltage | 0.75 | volt | Cell current density | 0.12 | A/cm$^2$ |
| | | | Nernst voltage ($E_{nerst}$) | 0.799 | volt |
| | | | Open circuit voltage | 0.919 | volt |
| | | | Steam temperature out | 1000 | °C |
| | | | Output power | 40.535 | kW |

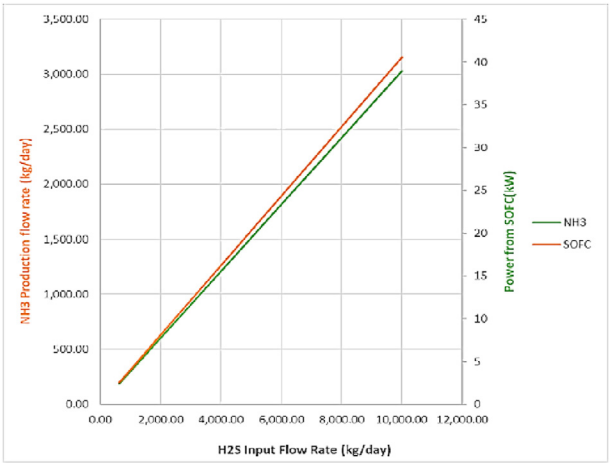


**Fig. 7 – The output energy from SOFC versus hydrogen sulfide flow rate fed to the EMS and ammonia produced.**

$$1/2O_2 + 2\,e^- \rightarrow 1/2O_2^{-2} \quad \text{(R8)}$$

Overall

$$H_2 + 1/2O_2 \rightarrow H_2O \quad \text{(R9)}$$

The results of our modelling (input and output data) are shown in Table 7. Cell temperature, ionic conductivity, and applied voltage were obtained from literature data such as Ramadhani et al. [38] and the values were selected specifically based on our design constraints. The cell area and thickness of the membrane are also subject to change. By changing the mentioned values in the input parameters, the following output results were obtained. 53.475 kg/day of hydrogen is required to produce 40.535 kW power. This hydrogen results from the separation of hydrogen sulfide in the EMS.

The relation between hydrogen sulfide input flow rate, ammonia produced, and power derived from the SOFC is shown in Fig. 7. The increase in the power derived from SOFC keeps pace with the ammonia flow rate. However, the generated power from SOFC is insignificant when compared to the ammonia production rate.

The total cell over-potential for both membranes and the fuel cell are calculated as shown in Eq. 5. $E_{eq}$ is the equilibrium over-potential, $\eta_{act}$ is the activation over-potential, $\eta_{conc}$ is the concentration over-potential, and $IR_{cell}$ is the ohmic over-potential.

$$E_{cell} = E_{eq} + \eta_{act} + \eta_{conc} + IR_{cell} \quad (5)$$

The required power, $P$, for running the separation processes is calculated based on Eq-6. (Area × current density) is

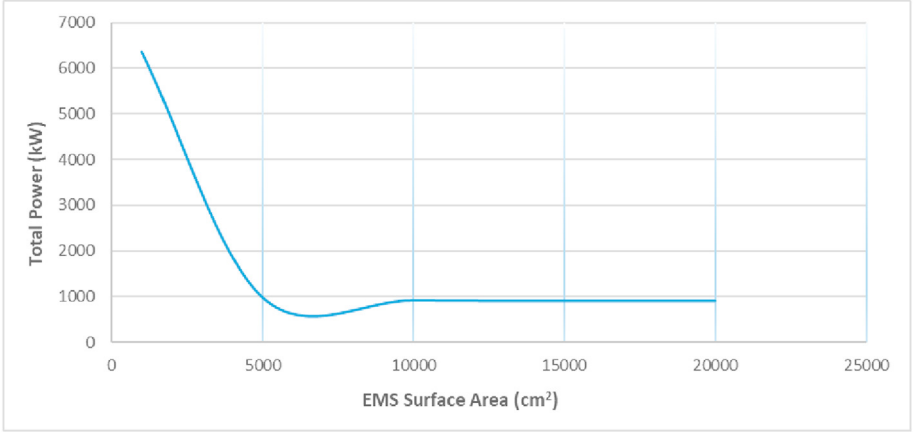


**Fig. 8 – The surface area required versus the energy consumption of the proposed process.**

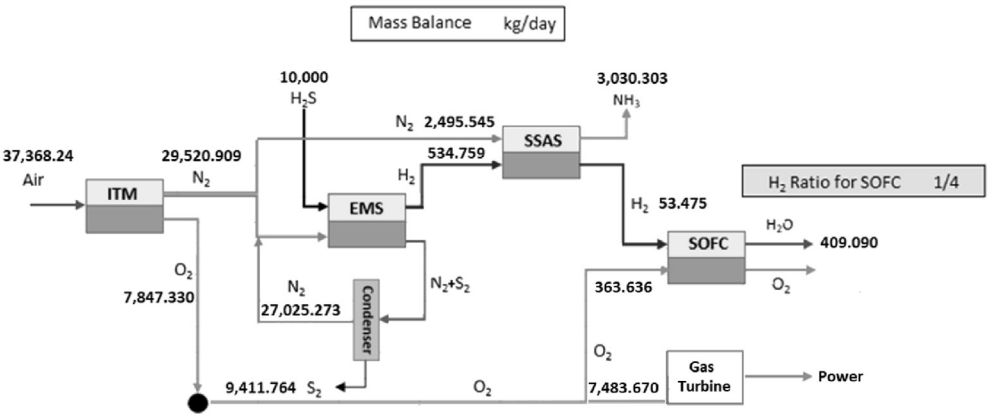


**Fig. 9 – A schematic of the mass balance of the proposed ammonia production process from hydrogen sulfide.**

**Table 8 – Mass-balance results of the proposed ammonia production process.**

| Mass balance of the proposed process (kg/day) | | | | | | | | |
|---|---|---|---|---|---|---|---|---|
| Elements | ITM | | EMS | | SSAS | | SOFC | |
| | Inputs | Outputs | Inputs | Outputs | Inputs | Outputs | Inputs | Outputs |
| Air | 37,368.24 | | | | | | | |
| $N_2$ | | 29,520.909 | 27,025.273 | | 2495.545 | | | |
| $O_2$ | | 7847.330 | | | | | | |
| $NH_3$ | | | | | | 3030.303 | | |
| $H_2S$ | | | 10,000 | | | | | |
| $H_2O$ | | | | | | | | 409.09 |
| $S_2$ | | | | 9411.764 | | | | |
| $H_2$ | | | | 588.235 | 534.759 | | 53.475 | |

the total current and V is the total voltage ($E_{cell}$ × number of cells).

$$P = I \times A \times V \tag{6}$$

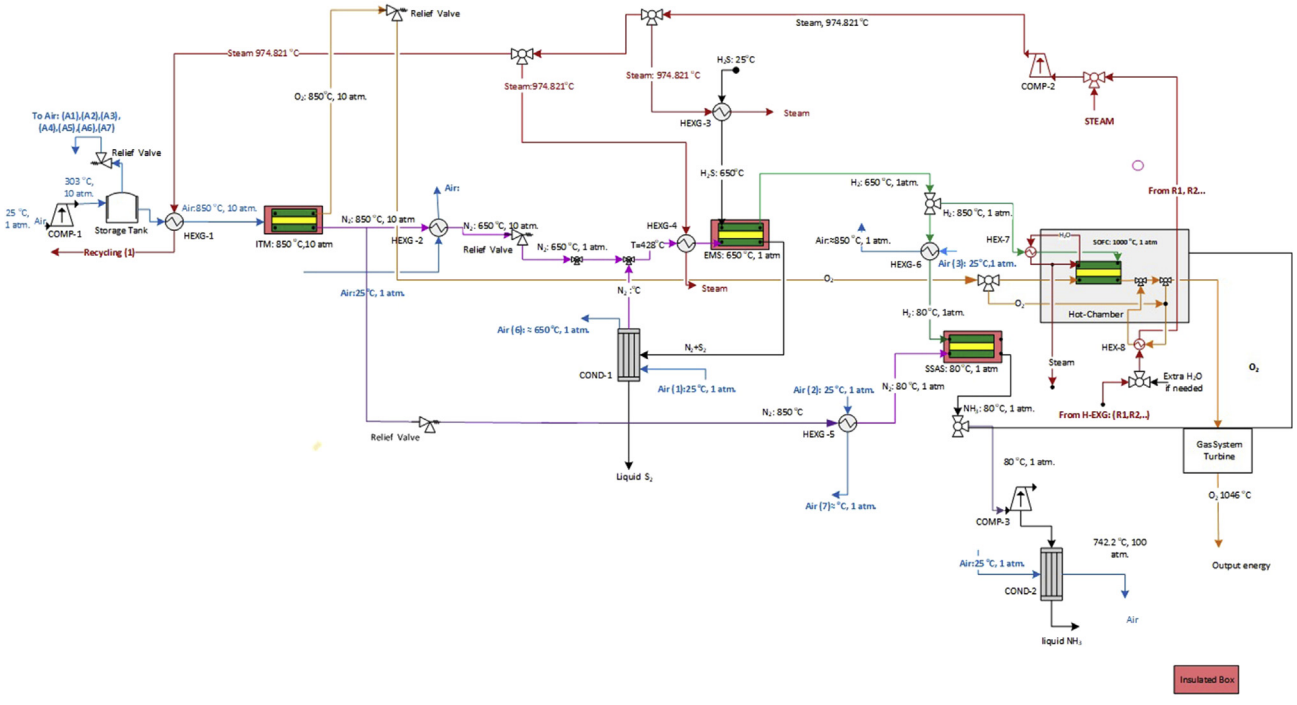


**Fig. 10 – A schematic of the energy flow diagram of the proposed ammonia production process.**

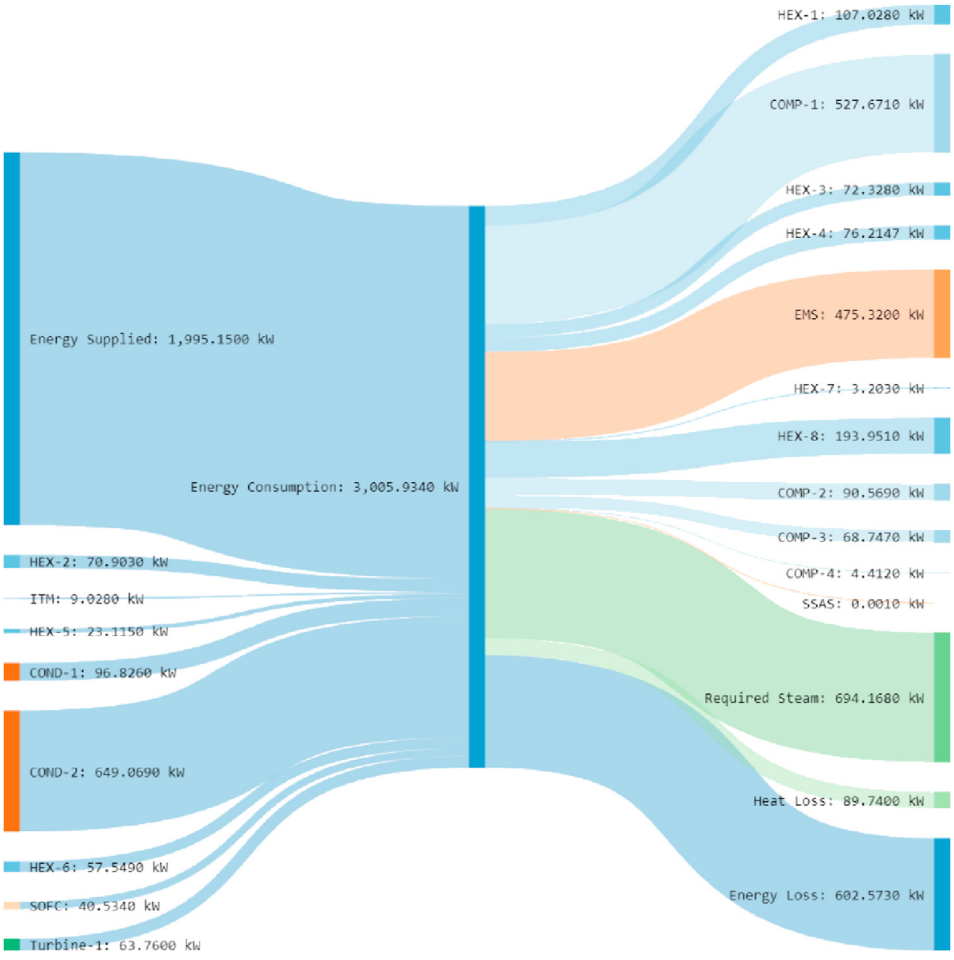


**Fig. 11 – Sankey diagram for input and output energy (based on Fig. 10).**

The relationship between the surface area ($cm^2$) of the EMS and power (kW) required for the proposed ammonia production process is shown in Fig. 8. This figure was obtained by giving various input values for the EMS surface area and running the simulated model to attain the total power output required for ammonia synthesis. As the surface area of the EMS increases, the total power of the proposed ammonia production process decreases. Between the surface area of 5000–10,000 $cm^2$, there is a turning point from which by increasing the surface area of the EMS, the total power increases until it levels off. The most suitable surface area for this proposed process is between 5000–10,000 $cm^2$, for which the total power is at its minimum. The empirical formula based on our simulated model shows that the relation between the EMS surface area ($cm^2$) to the total power required for operating the proposed ammonia production process (kW) is: $Y = 460950x^{-0.659}$.

## Mass balance results

A schematic of the mass balance of the proposed ammonia production process from hydrogen sulfide is shown in Fig. 9, while the results of the mass balance are shown in Table 8. This process has two inputs: air and hydrogen sulfide. 37.368 t of air flow rate enters the ITM for oxygen separation. The remaining 29.520 t nitrogen is split into two streams. 91.5% of the nitrogen enters the EMS as the sweep gas and the remaining is introduced into the SSAS for ammonia production. For the separation of the required hydrogen for ammonia synthesis, 10 t of hydrogen sulfide is introduced into the EMS. Approximately 91% of the separated hydrogen (534.759 kg) enters the SSAS and the remaining hydrogen along with about 5% of the separated oxygen from the ITM enters the SOFC for heat and power generation. The remaining 95% of the separated oxygen (7.483 t) enters into the gas turbine system for power generation. From the above-mentioned amount of hydrogen sulfide introduced into the EMS (10 t), 9.411 t of sulfur is separated and stored to be sold commercially.

## Energy balance results

Fig. 10 shows the energy flow diagram for the proposed process by means of heat integration. The need for external energy sources is minimized and heat recovery is maximized when the heat integration method is adopted. This process is cooled with the input air flow at 25 °C before entering the ITM and heated with the recirculated steam at 974.82 °C resulting from the SOFC at steady state conditions. The input air enters

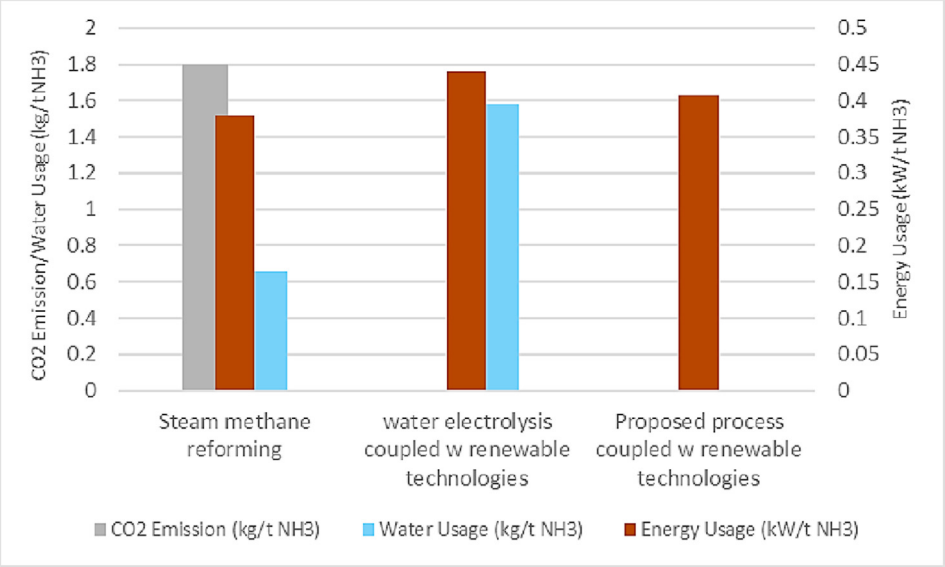


**Fig. 12 – A comparison of different ammonia production technologies in terms of $CO_2$ emissions, water, and energy consumption.**

a compressor in order to reach the desired pressure in the range of 10–30 atm before entering the ITM for oxygen separation. This air stream is heated from ambient temperature to 850 °C. The separated oxygen from the air stream enters a pressure reducing valve and reaches 1 atm. The separated oxygen is divided into two streams: the first stream enters the SOFC for heat and power production, while the second stream passes through the hot chamber where SOFC is located and goes through the compressor and turbine for power production. The remaining nitrogen from the input air stream after oxygen separation is cooled down with air before entering the SSAS at a pressure of 1 atm and temperature of 80 °C. The nitrogen from the ITM at a temperature of 850 °C is cooled down with air and lowered to 650 °C before entering the EMS as the sweep gas. Simultaneously, the hydrogen derived from the separation of hydrogen sulfide in the EMS enters the SSAS after being cooled with air to 80 °C. The resulting $N_2 + S_2$ from the EMS enters a condenser in order to separate nitrogen from sulfur. The separated nitrogen will then be recirculated back into the EMS as the sweep gas. The separated oxygen from the ITM at 850 °C along with a portion of the separated hydrogen from the EMS at 650 °C are heated to a temperature of 1000 °C before entering the SOFC for heat and power production.

The energy draw is driven primarily by the required steam which consumes 694.168 kW/day of power (Fig. 11). This is followed by the energy loss (602.573 kW/day), COMP-1 (394.32 kW/day), and power required for EMS (475.32 kW/day). Other energy uses are much smaller; indeed, the next highest energy use is the HEX-8 with 193.951 kW/day. A Sankey diagram based on the energy balance conducted is shown in Fig. 11.

### *A comparison of the proposed process with other available ammonia production technologies currently in use*

A comparison of the proposed ammonia production process with conventional methods (SMR and water electrolysis coupled with Haber-Bosch process) in terms of water usage (kg/t $NH_3$), $CO_2$ emissions (kg/t $NH_3$), and energy consumption (kW/t $NH_3$) at steady state conditions is shown in Fig. 12. This figure shows that the proposed ammonia process is the most efficient in terms of water consumption. SMR-Haber-Bosch (H–B) uses 0.66 kg $H_2O$/t $NH_3$ while water electrolysis shows an 82% higher consumption rate than SMR-H-B. In terms of removing $CO_2$ emissions, our process is similar to water electrolysis, assuming that both processes are powered by renewable technologies. However, the energy consumption of water electrolysis is 0.44 kW/t $NH_3$, which is approximately 15% higher than for SMR-H-B and 10% higher than for our proposed process. In conclusion, our proposed process reduces the energy usage compared to the water electrolysis process and reduces both $CO_2$ emissions and water usage.

## Conclusions

A novel process for ammonia production from hydrogen sulfide is proposed in this study. A mass and energy balance model have been developed by means of VBA software. The results show that the energy consumed in this process is high when compared to conventional methods, mostly due to the incorporation of EMS in the system. Based on the assumptions made and the selected operational conditions (temperature, pressure, and flow rate) and design elements for membranes (thickness, cell area, and applied voltage), this processing unit (EMS) needs 475.320 kW of power for its operation. For the production of approximately 3 t of ammonia, 1996.522 kWh energy and 10 t/day of hydrogen sulfide is required. The energy consumption of this process is almost 6.6% higher than that of SMR coupled with the Haber-Bosch process and approximately 8% lower than that of water electrolysis coupled with Haber-Bosch.

The main advantage of this proposed production process is that it directly converts hydrogen sulfide which is an

extremely harmful and toxic chemical compound into ammonia. This is accomplished through a process which is low carbon and consumes less water for its operation, unlike with a water electrolyzer and SMR-H-B. It has a small physical footprint due to utilization of compact membranes and fewer process steps when compared to competing processes (water electrolysis and SMR-H-B). Future studies should focus on reducing the energy consumption of the system by exploring the use of energy-efficient materials that lower the operational temperature and pressure of the EMS membranes.

## Declaration of competing interest

The authors declare that they have no known competing financial interests or personal relationships that could have appeared to influence the work reported in this paper.

## Acknowledgements

We wish to thank UKRI-BBSRC for funding to PS on grant BB/M011917/1, Renewable Fertilizer Production to Improve Agricultural Efficiencies & Avoid Environmental Harm. HG was a self-funded PhD Student. The authors wish to thank Ahmad G. Adl Tabatabai for his conceptual input on the model and Dr. Maria Vahdati and Daniel Cheung for their cooperation and help for editing the paper.

## REFERENCES

[1] UN. World Population Prospects. The 2015 revision, key findings and advance tables. working paper No. ESA/P/WP.241. 2015. New York, https://esa.un.org/unpd/wpp/publications/files/key_findings_wpp_2015.pdf. [Accessed 30 September 2020].
[2] Roberts TL. The role of fertilizer in growing the world's food. Better crops with plant food. International Plant Nutrition Institute (IPNI); 2009. https://www.ipni.net/ppiweb/bcrops.nsf/webindex/0022BBC19C02604A852575C50062FBB7/file/BC09-2p12.pdf. [Accessed 5 January 2018].
[3] Alexandratos N, Bruinsma J. World agriculture towards 2030/2050: the 2012 revision. Agricultural development economics division. Food and Agriculture Organization of the United Nations; 2012. http://www.fao.org/3/a-ap106e.pdf. [Accessed 30 September 2020].
[4] Soloveichik G. Future of ammonia production: improvement of Haber-Bosch process or electrochemical synthesis?. In: AIChE annu. Meet. Top. Conf. Minneapolis: NH3 Energy; 2017.
[5] CICE. The essential chemical industry. 2016. http://essentialchemicalindustry.org/chemicals/ammonia.html. [Accessed 30 September 2020].
[6] Matzen M, Alhajji M, Demirel Y. Technoeconomics and sustainability of renewable methanol and ammonia productions using wind power-based hydrogen. Adv Chem Eng 2015;5. https://doi.org/10.4172/2090-4568.1000128.
[7] Hughes T, Wilkinson I, Tsang E, McPherson I, Sudmeier T, Fellowes J, et al. Green ammonia. Cardiff, SIEMENS; 2015. http://businessdocbox.com/73271609-Green_Solutions/Green-ammonia-september-2015.html. [Accessed 30 September 2020].
[8] Garagounis I, Kyriakou V, Skodra A, Vasileiou E, Stoukides M. Electrochemical synthesis of ammonia in solid electrolyte cells. Front Energy Res 2014;2:1. https://doi.org/10.3389/fenrg.2014.00001.
[9] Wang L, Xia M, Wang H, Huang K, Qian C, Maravelias CT, et al. Greening ammonia toward the solar ammonia refinery. Joule 2018;2:1055–74. https://doi.org/10.1016/j.joule.2018.04.017.
[10] Parkinson B, Tabatabaei M, Upham DC, Ballinger B, Greig C, Smart S, et al. Hydrogen production using methane: techno-economics of decarbonizing fuels and chemicals. Int J Hydrogen Energy 2018;43:2540–55. https://doi.org/10.1016/j.ijhydene.2017.12.081.
[11] Breen K. Energy technology prospectives, pathways to a clean energy system. International Energy Agency (IEA); 2012. Paris, https://www.iea.org/publications/freepublications/publication/ETP2012_free.pdf. [Accessed 5 January 2018].
[12] Dincer I, Bicer Y. Ammonia production. In: Dincer I, editor. Compr. Energy syst. Elsevier; 2018. p. 42–82.
[13] Schnitkey G. Anhydrous ammonia, corn, and natural gas prices over time. Department of Agricultural and Consumer Economics, University of Illinois of Urbana-Champaign; 2016. Illinois, https://farmdocdaily.illinois.edu/2016/06/anhydrous-ammonia-corn-and-natural-gas-prices.html. [Accessed 30 September 2020].
[14] Cong L, Yu Z, Liu F, Huang W. Electrochemical synthesis of ammonia from N2 and H2O using a typical non-noble metal carbon-based catalyst under ambient conditions. Catal Sci Technol 2019;9:1208–14. https://doi.org/10.1039/c8cy02316f.
[15] Alcamo J, Flörke M, Märker M. Future long-term changes in global water resources driven by socio-economic and climatic changes. Hydrol Sci Sci Hydrol 2007;52. https://doi.org/10.1623/hysj.52.2.247.
[16] Ercin AE, Hoekstra AY. Water footprint scenarios for 2050: a global analysis. Environ Int 2014;64:71–82. https://doi.org/10.1016/j.envint.2013.11.019.
[17] Hoekstra AY, Chapagain AK, Aldaya MM, Mekonnen MM. The water footprint assessment manual. London (UK), Washington DC (USA): Earthscan; 2011. https://waterfootprint.org/media/downloads/TheWaterFootprintAssessmentManual_2.pdf. [Accessed 30 September 2020].
[18] Progressive Energy Ltd. The liverpool-manchester hydrogen cluster: a low cost, deliverable project (cadent). Technical Report. Stonehouse; 2017.
[19] Zhang Y, Peng L, Yu X. Protective effect of hydrogen sulfide on rats with myocardial ischemia/reperfusion injury and its mechanism. Chinese. 2015. PMID: 25744834, https://pubmed.ncbi.nlm.nih.gov/25744834/. [Accessed 30 September 2020].
[20] Mbah JC. Endurance materials for hydrogen sulfide splitting in electrolytic cell. Tampa: University of South Florida; 2008. https://scholarcommons.usf.edu/cgi/viewcontent.cgi?article=1386&context=etd. [Accessed 30 September 2020].
[21] Winnick J, Liu M. High temperature removal of H2S from coal gasification process streams using an electrochemical membrane system. Washington, D.C.: United States Government; 2003. https://www.osti.gov/servlets/purl/823016. [Accessed 30 September 2020].
[22] ATSDR. Agency. For toxic substances and disease registry. 2015. https://www.atsdr.cdc.gov/toxprofiles/tp114-c5.pdf. [Accessed 30 September 2020].
[23] dos Santos JPL, de Carvalho Lima Lobato AK, Moraes C, de Lima Cunha A, da Silva GF, dos Santos LCL. Comparison of different processes for preventing deposition of elemental

sulfur in natural gas pipelines: a review. J Nat Gas Sci Eng 2016;32:364–72. https://doi.org/10.1016/j.jngse.2016.04.045.
[24] Li H, Zhu L, Wang J, Li L, Shih K. Development of nano-sulfide sorbent for efficient removal of elemental mercury from coal combustion fuel gas. Environ Sci Technol 2016;50:9551–7. https://doi.org/10.1021/acs.est.6b02115.
[25] Bobbitt NS, Mendonca ML, Howarth AJ, Islamoglu T, Hupp JT, Farha OK, et al. Metal-organic frameworks for the removal of toxic industrial chemicals and chemical warfare agents. Chem Soc Rev 2017;46:3357–85. https://doi.org/10.1039/c7cs00108h.
[26] Wang H, Zeng X, Wang W, Cao D. Selective capture of trace sulfur gas by porous covalent-organic materials. Chem Eng Sci 2014;135:373–80. https://doi.org/10.1016/j.ces.2015.02.015.
[27] Porous liquid technologies. 2019. http://www.porousliquidtechnologies.com/. [Accessed 30 September 2020].
[28] Sun C, Larpudomlert R, Thepwatee S. Coal conversion and utilization for reducing CO2 emissions from a power plant. State College: Penn State University; 2011. https://personal.ems.psu.edu/~fkd/courses/egee580/2011/Final Reports/coal_igcc_report.pdf. [Accessed 30 September 2020].
[29] Xu G, Liu R, Wang J. Electrochemical synthesis of ammonia using a cell with a Nafion membrane and SmFe0.7Cu0.3-x Ni x O3 (x = 0-0.3) cathode at atmospheric pressure and lower temperature. Sci China, Ser B Chem 2009;52:1171–5. https://doi.org/10.1007/s11426-009-0135-7.
[30] Jimenez CA. Effect of composition, microstructure and component thickness on the oxidation behaviour of laves phase strengthened interconnect steel for Solid Oxide Fuel Cells (SOFC). Jülich: Forschungszentrum Jülich; 2014.
[31] Han L, Deng G, Li Z, Fan Y, Zhang H, Wang Q, et al. Simulation and optimization of ion transfer membrane air separation unit in an IGCC power plant. Appl Therm Eng 2018;129:1478–87. https://doi.org/10.1016/j.applthermaleng.2017.10.131.
[32] Marrony M. Proton conducting ceramics from fundamentals to applied research. Pan Stanford. Karlsruhe; 2015.
[33] Chemsystems. Air separation technology. San Francisco: Nexant Inc; 2010. https://www.nexantsubscriptions.com/file/41662/download?token=2w3gVnIV. [Accessed 30 September 2020].
[34] Burke A, Li S, Winnick J, Liu M. Sulfur-tolerant cathode materials in electrochemical membrane system for H2S removal from hot fuel gas. J Electrochem Soc 2004;151:D55. https://doi.org/10.1149/1.1758815.
[35] Amar IA, Lan R, Petit CTG, Tao S. Solid-state electrochemical synthesis of ammonia: a review. J Solid State Electrochem 2011;15:1845–60. https://doi.org/10.1007/s10008-011-1376-x.
[36] Lapina A, Holtappels P, Mogensen MB. Electrolytes and electrodes for electrochemical synthesis of ammonia. Kgs. Lyngby: Technical University of Denmark; 2013. https://backend.orbit.dtu.dk/ws/files/87560374/Electrolytes_and_Electrodes.pdf. [Accessed 30 September 2020].
[37] Abdalla AM, Hossain S, Azad AT, Petra PMI, Begum F, Eriksson SG, et al. Nanomaterials for solid oxide fuel cells: a review. Renew Sustain Energy Rev 2018;82:353–68. https://doi.org/10.1016/j.rser.2017.09.046.
[38] Ramadhani F, Hussain MA, Mokhlis H, Hajimolana S. Optimization strategies for solid oxide fuel cell (SOFC) application: a literature survey. Renew Sustain Energy Rev 2017;76:460–84. https://doi.org/10.1016/j.rser.2017.03.052.
[39] Uttamote T. Removal of CO2 and H2S from biogas for later application in solid oxide fuel cell. Thammasat University; 2011.